A 6 Year-Old Pediatric Finite Element Model for Simulating Pedestrian Impacts

Yunzhu Meng[1,3], Berkan Guleyupoglu[2,3], Bharath Koya[2,3], Scott Gayzik[2,3] , Costin D. Untaroiu[1,3]

1. Virginia Tech, 2. Wake Forest University School of Medicine
3. Virginia Tech-Wake Forest Center for Injury Biomechanics

Abstract

In addition to adult pedestrian protection, child pedestrian protection continues to be an important issue in vehicle crash safety. However, with exception of a child headform impact test, all other subsystem tests are designed for prediction of adult pedestrian injuries. The development of a computational child model could be a better alternative that characterizes the whole-body response of vehicle–pedestrian interactions and assesses the pedestrian injuries. Several pediatric pedestrian models have been developed but these existing models have several inherent limitations due to lack of biomaterial data. In this study, an advanced and computationally efficient finite element (FE) model corresponding to a six-year-old (6YO) pedestrian child was developed in LS-DYNA. The model was developed by morphing an existing GHBMC 5th percentile female pedestrian model to a 6-year old child geometry reported in literature. Material properties were applied based upon previously published studies. The standing posture has been used as specified in the EuroNCAP testing protocol. Component validations with simple impactor tests and a full-body validation in a car-to-pedestrian collision (CPC) were performed in LS-DYNA. Overall, the results of the model showed a reasonable correlation to the test data in component validations. The child pedestrian model showed also numerical stability under a typical CPC configuration. In addition, the most common injuries observed in pedestrian accidents including fractures of lower limb bones and ruptures of knee ligaments were predicted by the model. The child model will be further validated and then used by safety researchers in the design of front ends of new vehicles in order to increase pedestrian protection of children.

Introduction

Every year about 1.25 million people die as a result of road traffic crashes. In which, half of them are vulnerable road users: pedestrians, cyclists and motorcyclists [1]. World Bank predicts that the fatalities caused by road crashes in the world will increase by more than 65% between the years 2000 and 2020 if no pedestrian protection measures will be implemented worldwide [2]. According to National Highway Traffic Safety Association (NHTSA), 4,735 pedestrians were killed in the United States in 2015 by traffic collisions. It was also shown that child pedestrians are the most likely to be involved in a car to pedestrian collision (CPC) and pedestrian children from five to nine years old have the highest mortality rate among all pedestrians [3]. A six-year-old child is considered an appropriate representation of pre-pubescent children, so a dummy corresponding to this age is typically employed in development of pedestrian protection systems for children.

Pedestrian protection standards in new vehicle ratings have already been implemented in Asia and Europe. Several sub-system tests (head, upper leg, lower leg) are used in regulations and in the development of new technologies for adult pedestrian protection. However, only a headform impact test proposed by the European Enhanced Vehicle-safety Committee (EEVC) focuses on the pediatric injuries [4].

While protection of child pedestrians deserves more attention, it is difficult to scale adults to children because of differences in anthropometry and material properties. Both structural and material properties change during a child's growth. The skeleton develops from an elastic or rubbery material to a more rigid structure, and the physeal plate disappears when an infant grows

to an adult [5]. Thus, existing sub-systems designed for adult pedestrian protection may not be appropriate for children protection.

Computational finite element (FE) human models could be a better alternative to simulate the whole pedestrian-vehicle interaction and to investigate the injury mechanisms during CPC. Two pediatric pedestrian FE models corresponding to a six-year-old child [6] and a 10-year-old child [7] have been reported in literature. However, these existing models have inherent limitations at both the development and validation levels. Therefore, the main objective of this study was to develop an advanced and computationally efficient FE model of a six-year-old pedestrian child.

Model Development

The 6YO pedestrian model was developed by morphing existing simplified pedestrian models within the GHBMC family of models (M50 to F05, F05 to 6 YO). The M50 and F05 models were developed from subjects who were recruited to match target anthropometry for these body sizes. Radial basis function interpolation with a thin-plate spline as the basis function (RBF-TPS) was used with a relaxation algorithm to morph from a linear scaled version of the F05 model to the final target geometry [8]. The RBF-TPS method calculates thin-plate spline coefficients from landmark locations on reference and target geometries and applies the spline equations to the reference mesh to create the target mesh. An advantage of this method is that that it allows for the description of the target geometry, 6YO in this case, with a reduced set of landmark points. To obtain the morphed 6YO simplified pedestrian model using the RBF-TPS morphing method, the source model's node information along with homologous landmarks between the reference and target geometries were used as inputs. After an initial morph using an altered version of 6 year old seated CAD surfaces [9], anthropometry was compared to gross values in the literature [10] to verify accuracy of the morph. Retrospective scan data were used to locally adjust the geometry as needed for accuracy, e.g. in the C-spine. The initial morphed model[11] was found to underestimate the target mass of 23.4 kg[12].

A second morphing process was performed to achieve a more anthropometrically accurate body shape, using data from the recent statistical geometry [13]. Once again the RBF-TPS method was used. The RBF-TPS morphing method generated a quality mesh with over 98% of elements passing hard targets set by the GHBMC prior to post-morph mesh adjustments. The elements below quality thresholds were edited manually to achieve 100% agreement with GHBMC program targets.

The pedestrian model has a mass of 27 kg and height of 117 cm. Several anthropometric measures were calculated and compared with the corresponding standards measures [14]. As shown in Table 1, the model anthropometry data showed to be in good agreement with literature data.

Table 1. Comparison between some anthropometric measures between the model and literature standard

	FE Model (cm)	ASTM Standard (cm)
Waist Girth	60.0	58.4
Thigh Girth	38.3	36.2
Knee Girth	27.9	25.1
Ankle Girth	18.2	17.8

The final model has 545,616 nodes, 834,734 elements and 596 parts. Table 2 shows the quality of elements compared to criteria suggested by the GHBMC. Overall, there was a high quality among the elements with 99.9% of them within allowable limits.

Table 2. The model mesh quality

	Quality Criterion	Min. value	Max. value	Allowable limit	Nr. of elements under allowable limit (%)
Shell Elements	Jacobian	0.141	1	0.3	125(0.06%)
	Warpage	0	59.6	50	159(0.08%)
	Aspect Ratio	1	10.1	8	15(0.008%)
Solid Elements	Jacobian	0.3		0.3	0(0%)
	Warpage		120.38	50	2323(0%)
	Aspect Ratio	1.031	20.48	8	726(0%)

Model Validation

In a typical CPC accident, a pedestrian is usually impacted laterally by the vehicle front end. Pedestrian's lower extremities are first impacted by the bumper and are accelerated rapidly while the head and torso keep almost the same location. Then, pedestrian's thighs and pelvis are impacted by the vehicle hood edge and pedestrian's torso wraps around the hood. Finally the vehicle-to pedestrian interaction ends with the head impacting to the hood and/or the windshield. [15]. Current pedestrian safety measures try to reduce the stiffness of the car parts which come into contact with the pedestrian in order to reduce the injury risk. However, the vehicle-to-pedestrian interaction is complex, so a human FE model may capture better the whole interaction, help to understand the injury mechanisms, and improve vehicle design.

As with other human FE models, the child pedestrian model requires component and full body validations against post-mortem human surrogate (PMHS) data to increase the confidence in its predictions before being used in various applications. The child model was validated against a very few child component tests identified in literature. These PMHS tests and corresponding FE simulations are described in the following sections.

Model Validation of Femur under Anterior-Posterior (AP) Bending Loading

In testing, two 6 YO PMHS femurs were loaded under lateral bending using a universal testing machine (SWD-10). The bone ends were potted in cups and an impactor loaded the femur at mid-shaft location with a constant velocity (0.5 m/min) [16]. Little information was provided about the test setup (e.g. potting material properties, cup dimensions, etc.), so the bending of 6YO femur FE model (Fig. 1) was simulated under simplified conditions. The distal and proximal femoral ends were supported on two rigid parts, and an impactor model loaded the femur at its middle location with the same velocity as in testing. Initially, the femur material properties corresponding to 50th male FE model [17, 18] were assigned to the 6 YO FE model. Since the femur model showed to have higher stiffness and failure force, a literature review was performed to identify the pediatric femoral material properties. The values of Young's elastic modulus obtained by testing pediatric femoral specimens were reported in literature [19]. Additionally, a Young's modulus vs. age curve was fitted and published[20]. Based on above literature review, a Young's modulus of 9 GPa was assigned to the 6 YO pedestrian's femoral cortical bone. Since no values of femoral yield stress were identified in literature for pediatric population, the yield stress was considered to change proportionally to Young's moduli, so a value of 70.8 MPa was assigned as yield stress. Finally, it was assumed that both adult and child cortical bone have the same failure plastic strain (0.8 %). The AM bending simulation was performed in LS-Dyna® software (LSTC, Livermore, CA, USA) using an implicit solver (v.R712). To avoid the compression fracture between the impactor and the bone, the failure criteria was not defined in the femur elements under the impactor.
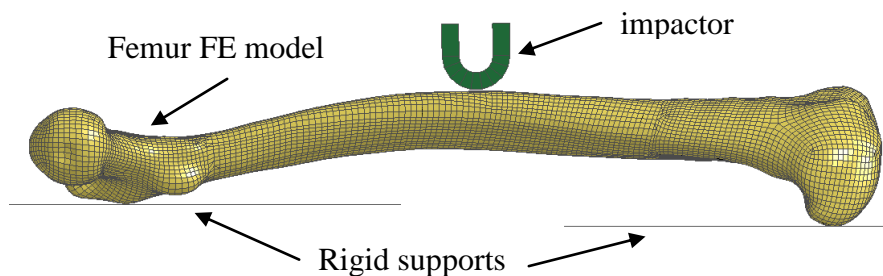

Figure 1. The Setup of the three point bending simulation

Model Validation under Lateral Loading

Overall, the pelvis anatomy of children is similar to adults. However, due to some differences in epiphyseal growth centers and apophyseal growth regions, the child's pelvic bone is softer and could absorb more energy during crash. [21].

The pelvic region of 6YO pedestrian FE model was validated against PMHS data recorded in lateral impact tests. Two six-year-old PMHS were impacted laterally using a square impactor at two different constant speeds (7.1 m/s and 7.7 m/s). The impactor has the weight of 3.24 kg, and size 18 X 14 cm. A wall was set close to body, so that the body was restrain to move. No fractures were recorded during tests[22].

Specific details about the materials used for experimental equipment were not provided, so the impactor, the wall and the ground were defined as rigid materials in the FE simulation. The impactor was positioned at the pedestrian pelvis. The FE model was positioned in standing position and impacted from right side with the impactor positioned at the middle of pelvis.
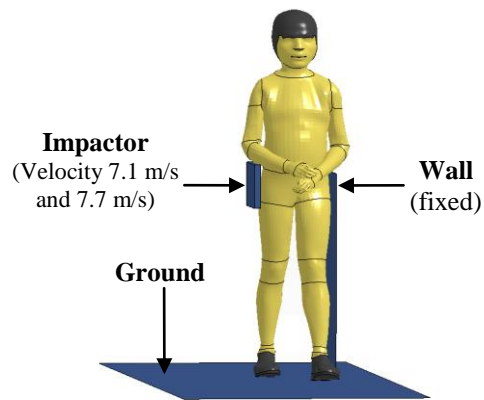
Figure 2. The Setup of the lateral pelvic impact test

Car-to-Pedestrian Impact Simulation

The stability of the pedestrian child FE model was verified in a CPC simulation under initial conditions similar to those used in adult PMHS pedestrian impact tests [23, 24]. To mimic the PMHS tests, the child FE model was positioned laterally at the vehicle's centerline in a mid-stance gait posture (Fig.3). As in the previous CPC simulation with a 50th male pedestrian FE model [25], gravity was assigned to the pedestrian model and a force corresponding to its weight were applied upward by the ground model about 8-ms <u>before the impact</u> (Fig.3).
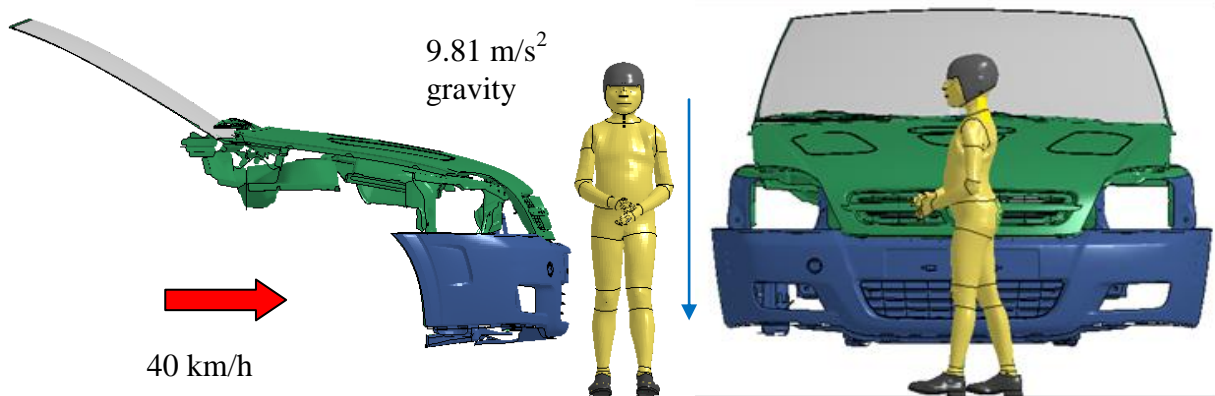

Figure 3. The initial position of the child pedestrian relative to the mid-sedan vehicle

A mid-sedan FE model corresponding to the vehicle used in adult PMHS pedestrian tests [23] was assigned a 40 km/h initial velocity. Appropriate contacts were assigned between pedestrian, as well as the vehicle and pedestrian parts. While CPC impact data is currently lacking in literature, the model stability and overall behavior during the CPC simulation were verified. In addition, the injuries predicted by the model were investigated.

Results and Discussion

Component Validations

Dynamic three-point bending tests were performed on the 6YO's femur FE model using both adult and child material properties. The femur fracture occurred on the opposite side of the femur region loaded by impactor, the zone which experienced the highest tension stress (Fig. 4a). However, it should be mentioned that failure was not defined in the region under the impactor to avoid artefactual compression fractures predicted by the elastic-plastic material model (MAT_3, LS-Dyna Manual) symmetric in tension and compression used in the original model[17]. It is well known that the cortical bone has a higher stiffness and strength in compression than in tension. However, an accurate material model which could capture this behavior together with the strain-rate dependency is missing in LS-DYNA. Therefore, future studies should focus on improving LS-DYNA material model library.

The femur with assumed pediatric properties showed less stiffness and lower fracture force than the similar model with adult material properties [17]. Although the child stiffness curves were not published, the corresponding simulation curve showed a similar linear shape as that reported in adult tests[26]. Fracture occurred in the two PMHS tests at 719 N and 1459 N. The individual variation in the failure force could be caused by PMHS stature, weight and cause of death [16]. The failure force recorded by the FE model with child material properties (Fig. 4b) was 1,500 N close to the highest PMHS data. While more documented tests on child femur specimens are recommended to be performed in the future, the promising results obtained here with the child femur suggest it can be used in vehicle-to-child pedestrian simulations.
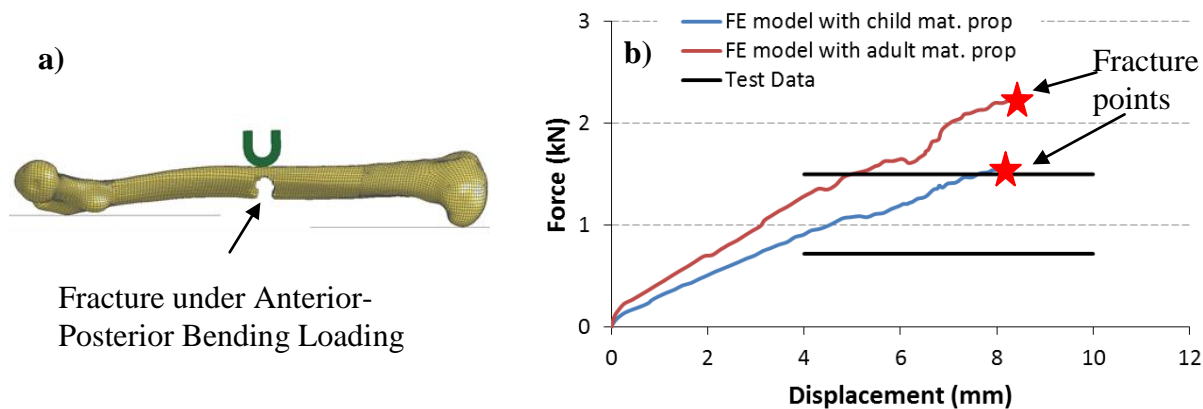

Figure 4. The femur fracture under Anterior-Posterior (AP) bending loading (a) The femoral AP bending stiffness curves: Comparison between the FE model with adult and child material properties

Lateral Loading Validation

As in the testing, no fractures were predicted during the pelvic region for both lateral loading simulations with 7.1 m/s and 7.7 m/s initial velocities. The time histories of both impact force and the Viscous Criterion (V*C) predicted by the model showed qualitatively the same trend as the corresponding test data (Fig. 5-6). Since a better correlation to test data [16] was recorded during the simulation with lower impact velocity, the rate-dependency of the pelvic region may play a significant role in this impact tests. In addition, the energy dissipated by the model in both simulations was lower than in testing. The differences between the results of tests and simulations could be caused by possible inaccuracies in child anthropometry, initial position

of impactor, and material properties of pelvic parts. Therefore, more tests on child PMHS are suggested to be performed with recording more accurately the test conditions. In addition, the strain-rate dependency of the model should be reviewed and eventually updated when appropriate test data will be identified in literature.
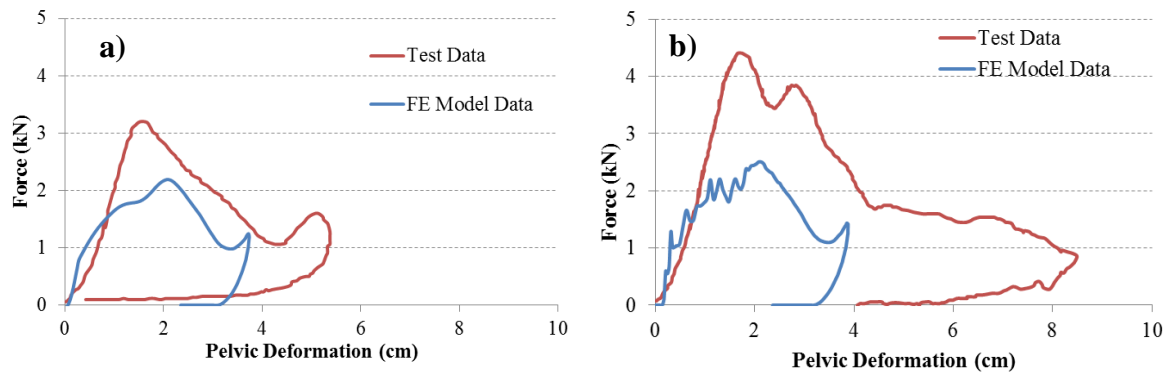

Figure 5. The force-pelvic deformation curves: FE results vs. Test Data. 7.1 m/s impact test (a) 7.7 m/s impact test (b).
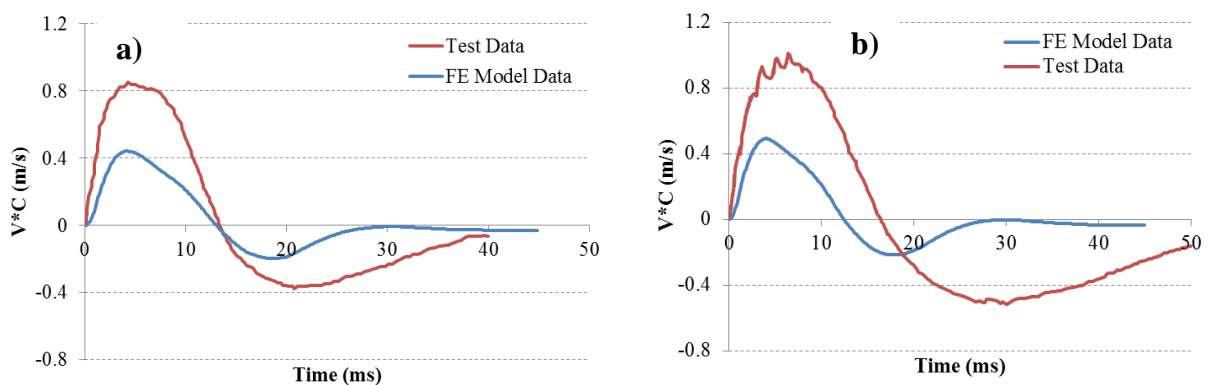

Figure 6. V*C time histories curves: FE results vs. Test Data. 7.1 m/s impact test (a) 7.7 m/s impact test (b).

Car-to-Pedestrian Impact simulation

The pedestrian child model showed numerical stability under the same tested CPC configuration (Fig. 7) as our previous child model [11]. The initial contact between the car and the child right lower limb occurs at about 8ms. The right femur is impacted by the upper region of the bumper and a fracture of the proximal femoral shaft is predicted at about 17ms. Then, the right knee is loaded under valgus bending by the bumper and a Medial Collateral Ligament (MCL) failure is observed (Fig. 8). It should be mentioned that the MCL failure under combined Lateral-Medial (LM) valgus bending and shear loading was also observed in the PMHS knee tests [27], and it is well recognized as a major injury mechanism of knee under lateral impact. As the car front end loads the left lower limb, a Lateral Collateral Ligament (LCL) failure occurs in the left knee due to the combined Medial-Lateral (ML) valgus bending and shear loading. Finally, the pedestrian's body wrapped around the vehicle front and a head-to-car hood impact was observed at about 78ms.

time = 10 ms   time =20 ms   time =40 ms

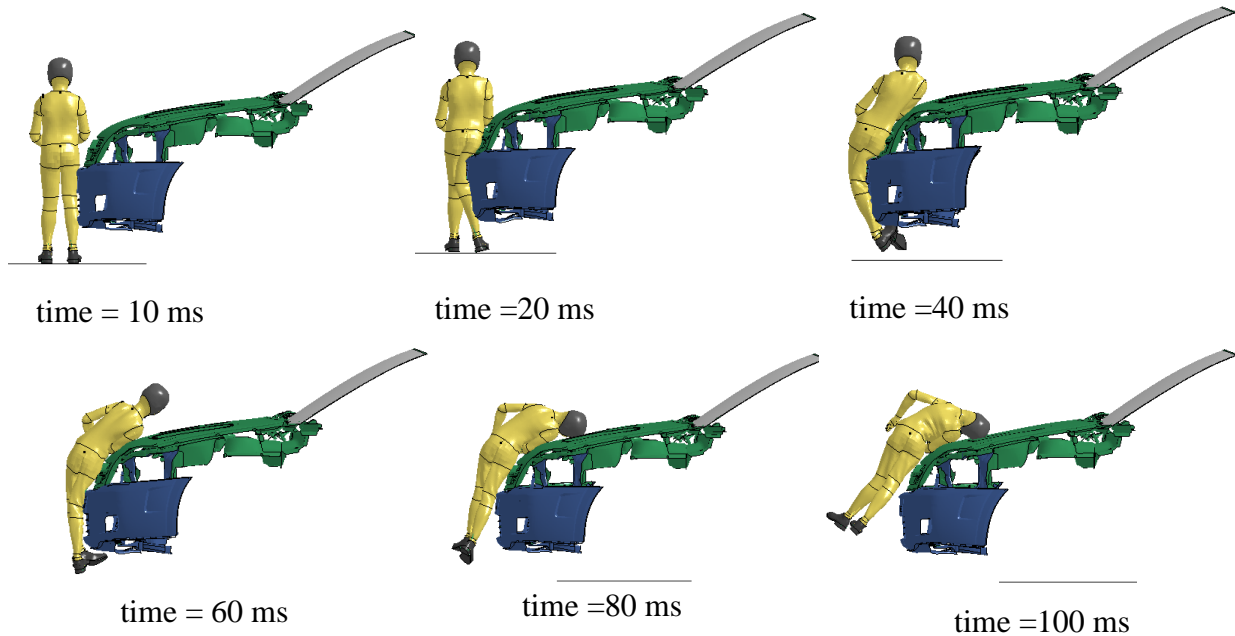time = 60 ms   time =80 ms   time =100 ms

Figure 7. The Pedestrian Kinematics during the CPC Impact Simulation

Overall, the child pedestrian model predicted the most common injuries observed in pedestrian accidents, but more confidence could be added to the model by further model improvements and validations. Improvements could be made to the model mesh by adding more parts which were neglected in these models (e.g. muscles, other ligaments) and especially to material properties. While majority of material properties of child parts were assumed, material tests on child parts especially in the lower limb region are recommended to be performed in the future. Finally, model validation of the full child pedestrian model based on real-world accident data is also highly recommended [26].
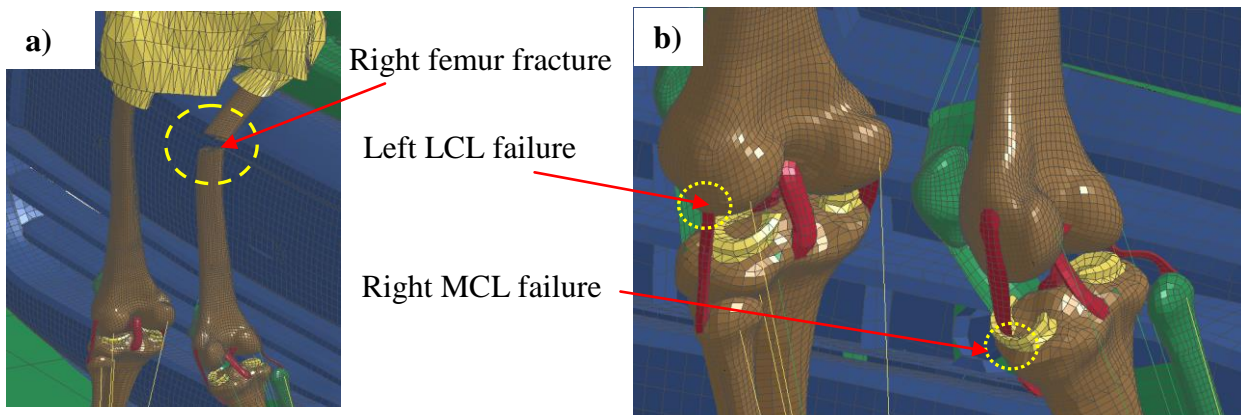

Figure 8. The Lower Limb injuries predicted by the Pedestrian Model during CPC Impact Simulation. Femoral fracture (a), knee ligament failure (b)

Acknowledgements

References

[1] WHO. (2015). *Road Traffic Injuries (October 2015 ed.)*. Available: http://www.who.int/mediacentre/factsheets/fs358/en/

[2] T. Bliss. (2014, April). *Implementing the Recommendataions of The World Report on Road Traffic Injury Prevention*. Available: http://www-wds.worldbank.org/external/default/WDSContentServer/WDSP/IB/2004/06/29/000112742_20040629103242/Rendered/PDF/295570tn11.pdf

[3] NHTSA. Traffic Safety Facts 2013 Data [Online].

[4] EEVC. Improved Test Methods to Evaluate Pedestrian Protection Afforded by Passenger Cars [Online].

[5] N. E. Green and M. F. Swiontkowski, *Skeletal Trauma in Children*, 1994.

[6] M. Okamoto, Y. Takahashi, F. Mori, M. Hitosugi, J. Madeley, J. Ivarsson*, et al.*, "Development of finite element model for child pedestrian protection," in *Proceedings of the 18th International Conference on the Enhanced Safety of Vehicles (ESV)*, 2003.

[7] L. Dong, G. Li, H. Mao, S. Marek, and K. H. Yang, "Development and validation of a 10-year-old child ligamentous cervical spine finite element model," *Ann Biomed Eng,* vol. 41, pp. 2538-52, Dec 2013.

[8] N. A. Vavalle, S. L. Schoell, A. A. Weaver, J. D. Stitzel, and F. S. Gayzik, "Application of Radial Basis Function Methods in the Development of a 95th Percentile Male Seated FEA Model," *Stapp Car Crash J,* vol. 58, pp. 361-84, Nov 2014.

[9] M. Reed, M. Lehto, L. Schneider, and S. Moss, "Development of Anthropometric Specifications for the Six-Year-Old OCATD," 2001.

[10] R. G. Synder, L. W. Schneider, C. L. Owings, H. M. Reynolds, D. H. Golomb, and M. A. Schork, "Anthropometry of Infants, Children and Youths to Age 18 for Product Safety Design," presented at the Consumer Product Safety Commission, 1977.

[11] C. D. Untaroiu, J. Schap, and S. Gayzik, "A Finite Element Model of a 6-Year-Old Child for Simulating Pedestrian Impacts," *Traffic Injury Prevention,* vol. 16, pp. S257-S258, Oct 8 2015.

[12] *HYBRID III 6-Year Old Physical Data*. Available: http://www.nhtsa.gov/Research/HYBRID+III+6-Year+Old+Physical+Data

[13] B. K. Park and M. P. Reed, "Parametric body shape model of standing children aged 3-11 years," *Ergonomics,* vol. 58, pp. 1714-25, Oct 2015.

[14] A. S. f. T. a. Materials. ASTM Standards for Body Measurements [Online].

[15] J. L. Martin, A. Lardy, and B. Laumon, "Pedestrian Injury Patterns According to Car and Casualty Characteristics in France," *Ann Adv Automot Med,* vol. 55, pp. 137-46, 2011.

[16] J. Ouyang, Q. Zhu, W. Zhao, Y. Xu, W. Chen, and S. Zhuong, "Biomechanical Character of Extremity Long Bones in Children and Its Significance," *Chinese Journal of Clinical Anatomy,* vol. 21, p. 4, 06.31.2003 2003.

[17] C. D. Untaroiu, N. Yue, and J. Shin, "A Finite Element Model of the Lower Limb for Simulating Automotive Impacts," *Annals of Biomedical Engineering,* vol. 41, pp. 513-526, Mar 2013.

[18]   N. Yue and C. D. Untaroiu, "A Numerical Investigation on the Variation in Hip Injury Tolerance With Occupant Posture During Frontal Collisions," *Traffic Injury Prevention,* vol. 15, pp. 513-522, Jul 4 2014.

[19]   J. Currey and G. Butler, "The mechanical properties of bone tissue in children," *The Journal of Bone & Joint Surgery,* vol. 57, pp. 810-814, 1975.

[20]   B. J. Ivarsson, J. R. Crandall, D. Longhitano, and M. Okamoto, "Lateral injury criteria for the 6-year-old pedestrian-Part II: Criteria for the upper and lower extremities," SAE Technical Paper 0148-7191, 2004.

[21]   N. E. Green and M. F. Swiontkowski, *Skeletal trauma in children* vol. 3: Elsevier Health Sciences, 2009.

[22]   J. Ouyang, Q. Zhu, W. Zhao, Y. Xu, W. Chen, and S. Zhong, "Experimental cadaveric study of lateral impact of the pelvis in children," *Di 1 jun yi da xue xue bao= Academic journal of the first medical college of PLA,* vol. 23, pp. 397-401, 408, 2003.

[23]   J. R. Kerrigan, J. R. Crandall, and B. Deng, "A comparative analysis of the pedestrian injury risk predicted by mechanical impactors and post mortem human surrogates," *Stapp Car Crash J,* vol. 52, pp. 527-67, Nov 2008.

[24]   C. Untaroiu, J. Kerrigan, C. Kam, J. Crandall, K. Yamazaki, K. Fukuyama*, et al.*, "Correlation of strain and loads measured in the long bones with observed kinematics of the lower limb during vehicle-pedestrian impacts," *Stapp Car Crash J,* vol. 51, pp. 433-66, Oct 2007.

[25]   C. D. Untaroiu, J. B. Putnam, J. Schap, M. L. Davis, and F. S. Gayzik, "Development and Preliminary Validation of a 50th Percentile Pedestrian Finite Element Model," in *ASME 2015 International Design Engineering Technical Conferences and Computers and Information in Engineering Conference*, 2015.

[26]   C. D. Untaroiu, "A numerical investigation of mid-femoral injury tolerance in axial compression and bending loading," *International Journal of Crashworthiness,* vol. 15, pp. 83-92, 2010.

[27]   D. Bose, K. S. Bhalla, C. D. Untaroiu, B. J. Ivarsson, J. R. Crandall, and S. Hurwitz, "Injury tolerance and moment response of the knee joint to combined valgus bending and shear loading," *Journal of Biomechanical Engineering-Transactions of the Asme,* vol. 130, Jun 2008.